Spin-glass state induced by cobalt substitution in $CaRuO_3$

2007 J. Phys.: Condens. Matter 19 216212

(http://iopscience.iop.org/0953-8984/19/21/216212)

IOP PUBLISHING JOURNAL OF PHYSICS: CONDENSED MATTER

J. Phys.: Condens. Matter **19** (2007) 216212 (13pp) doi:10.1088/0953-8984/19/21/216212

Spin-glass state induced by cobalt substitution in $CaRuO_3$

Y Bréard[1], V Hardy[1], B Raveau[1], A Maignan[1], H-J Lin[2], L-Y Jang[2], H H Hsieh[3] and C T Chen[2]

[1] Laboratoire CRISMAT, UMR 6508 CNRS ENSICAEN, Boulevard du Maréchal Juin, 14050 Caen Cedex 4, France
[2] National Synchrotron Radiation Research Center, 101 Hsin-Ann Road, Hsinchu 30076, Taiwan
[3] Chung Cheng Institute of Technology, National Defense University, Taoyuan 335, Taiwan

Received 8 January 2007
Published 27 April 2007
Online at stacks.iop.org/JPhysCM/19/216212

Abstract

This paper reports on an experimental study of the effects induced by the substitution of Co for Ru in $CaRuO_3$, a prototypical oxide close to a magnetic instability. The $L_{2,3}$ x-ray absorption spectroscopy (XAS) spectra of Ru and Co in $CaRu_{1-x}Co_xO_3$ reveal that Co is in a divalent state for low x values, while the Ru valence increases upon increasing the Co content. The dc and ac magnetic susceptibilities demonstrate that the $CaRu_{1-x}Co_xO_3$ compounds can be classified as spin glasses. The origin of this behaviour and its implications are discussed. The effect of Co is also compared with the literature about substitutions by other cations in the magnetic sublattice of $CaRuO_3$.

1. Introduction

The nature of the magnetic state of $CaRuO_3$ is a long-standing subject of controversy in the physics of oxides [1–9]. Even though the debate is still intense, an agreement is emerging about the fact that this compound would be *on the verge of a ferromagnetic instability* [3, 5, 10]. Accordingly, one can expect that a variety of perturbations—such as small levels of substitutions—are able to profoundly affect the magnetic ground state of $CaRuO_3$.

In fact, several recent studies have reported that a ferromagnetic (FM) state can be created by substitutions in the Ru sublattice, even for concentrations lower than 5%. Up to now, five transition metals (M) were found to yield such an FM state in $CaRu_{1-x}M_xO_3$: Ti [11–13] Fe [12, 14, 15], Ni [14], Mn, [14] and Cr [16, 17]. As for the other substituting elements investigated so far, they all led to less clear situations, which were most often qualitatively described in terms of short-range magnetic ordering [14, 18]. There is a series of three elements, however, for which the possible achievement of a spin-glass (SG) state has been suggested.

With M = Sn, an SG state was claimed to take place in a restricted range of x values ($0.04 \leqslant x \leqslant 0.10$) [3]. This conclusion was based on qualitative features of the zero-field-cooled (ZFC) and field-cooled (FC) dc magnetic susceptibility: first, the ZFC $\chi_{dc}(T)$ curve

exhibits a peak; second, the FC and ZFC curves diverge from each other below the temperature of this peak.

With M = Cu, an SG was claimed to take place for $x \leqslant 0.07$, a statement also inferred from the behaviour of the ZFC/FC dc magnetic susceptibility [19].

With M = Co, the FC $\chi_{dc}(T)$ recorded in 1 T for $x = 0.25$ was found to exhibit a cusp, which was considered to be suggestive of a spin-glass transition [14].

It is worth noting that, in all cases, the occurrence of an SG state was only supported by the behaviour of the ZFC/FC $\chi_{dc}(T)$ curves. Even though such features are indeed consistent with an SG state, we emphasize that they cannot be regarded *per se* as experimental evidence for the formation of a spin glass. For instance, very similar sets of ZFC/FC curves can be observed in some ferromagnets, in which the peaked shape of the ZFC susceptibility results from the progressive alignment of randomly oriented ferromagnetic domains. It turns out that this is in particular the case of ferromagnetic $CaRu_{1-x}M_xO_3$ compounds, e.g. with M = Ti [12, 13] or Fe [12]. In fact, the metastable character of a spin glass generates other experimental signatures which are more specific of this magnetic state [20]. The best-known example is the frequency dependence of the in-phase and out-of-phase ac susceptibility, a type of characterization which, however, was not carried out in the previous investigations reporting a possible SG state in $CaRu_{1-x}M_xO_3$.

Therefore, the goal of the present work was to address in more detail the question of a substitution-induced spin-glass state in $CaRu_{1-x}M_xO_3$, by combining measurements of ac and dc magnetic susceptibility. Among the three substituting elements for which presumptions of an SG state already exist (i.e. Sn, Cu and Co), we chose to re-investigate the case of M = Co, which was the one that was the least documented.

2. Experimental details

$CaRu_{1-x}Co_xO_3$ samples ($0.1 \leqslant x \leqslant 0.5$) were prepared from intimate mixtures of CaO, RuO_2 and Co_3O_4 oxides, in stoichiometric proportions. The resulting powder was pressed in the form of bars and placed in platinum crucibles. The bars were then heated up to 1300 °C in air with a speed rate of 3 °C min^{-1}, maintained at this temperature for 12 h, and slowly cooled down to room temperature at the same rate.

X-ray powder diffraction (XRPD) patterns were collected over an angular range $5° < 2\theta < 120°$ with an X'pert Pro diffractometer working with the Cu Kα radiation. These data were used to check the purity of the compounds and to refine their lattice cell parameters.

Samples for transmission electron microscopy (TEM) were crushed in *n*-butanol and small flakes were deposited on a holey carbon film supported by a copper grid. The electron diffraction (ED) investigation was carried out with a 200 kV, JEOL 200CX microscope, tilting around the crystallographic axes. This microscope is equipped with an energy dispersive spectroscopy (EDS) analyser.

Soft x-ray absorption spectroscopy (XAS) experiments were carried out at the National Synchrotron Radiation Research Center (NSRRC, Taiwan), in order to investigate the valence state of Co and Ru. The Ru-$L_{2,3}$ spectra were measured at the 15B beamline, equipped with a double Si(111) crystal, while the Co-$L_{2,3}$ spectra were measured at the Dragon beamline. The photon energy resolution was set to 0.8 eV at the Ru-$L_{2,3}$ edges ($h\nu \cong 2.9$ keV) and to 0.5 eV at the Co-$L_{2,3}$ edges ($h\nu \cong 790$ eV). All spectra were recorded using the total electron yield method in a chamber with a base pressure in the high 10^{-10} mbar range. Clean sample areas were obtained by cleaving the crystals *in situ*. The first sharp peak at 777 eV of photon energy at the Co-L_3 edge of a CoO sample allowed an energy calibration better than 50 meV.

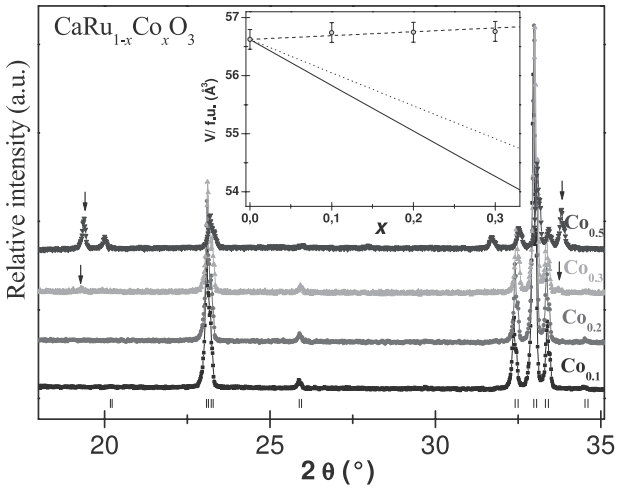

Figure 1. X-ray powder diffraction patterns of $CaRu_{1-x}Co_xO_3$ for $0 \leqslant x \leqslant 0.5$. Vertical bars at the bottom indicate peaks position based on the *Pnma* space group for $CaRuO_3$. Arrows indicate peaks belonging to the secondary phase which appears for $x \geqslant 0.3$. Inset: cell volume versus cobalt content, along with the theoretical variations expected when considering different cationic compositions: $CaRu^{4+}_{1-x}Co^{4+}_xO_3$ (solid line); $Ca[Ru^{4+}_{1-3x}Ru^{5+}_{2x}]Co^{2+}_xO_3$ (dashed line); $Ca[Ru^{4+}_{1-2x}Ru^{5+}_x]Co^{3+}_xO_3$ (dotted line).

A superconducting quantum interference device (SQUID) magnetometer (MPMS 5 T, Quantum Design) was used to measure the low-field dc susceptibility (χ_{dc}) in the ZFC and FC modes, as well as the in-phase (χ') and out-of-phase (χ'') ac susceptibility, at frequencies (f) between 0.1 and 1000 Hz. These measurements were complemented by means of another extraction magnetometer (PPMS 9 T, Quantum Design), allowing us to increase the frequency range up to 10 000 Hz.

3. Results and discussion

3.1. Structure

The solid solution $CaRu_{1-x}Co_xO_3$ was studied for $0 \leqslant x \leqslant 0.5$. After the thermal treatment described above, all products appeared as black sintered bars. The XRPD study showed that the compounds are single phase for x up to 0.2. For $x \geqslant 0.3$, however, a secondary phase was systematically observed, with an amount increasing with x (see figure 1). Therefore, the present paper will be mainly focused on the range $x < 0.3$, most attention being paid to the compound $CaRu_{0.8}Co_{0.2}O_3$ which corresponds to the highest cobalt content yielding a single phase. It must be specified, however, that the extra phase can be easily distinguished from the main one on the XRPD patterns, owing to a marked difference between the typical set of peaks associated with each of these structures.

All the peaks of the main phase were indexed in the classical cell characteristic of the $CaRuO_3$ structure: $a \approx c \approx a_p\sqrt{2}$ and $b \approx 2a_p$, space group *Pnma* (a_p is for the ideal parameter of the perovskite). Since the TEM study did not reveal any long-range cationic ordering, the refinements of the cell parameters were performed with Ru and Co occupying the same crystallographic site. Such a statistic distribution of the transition metals is supported by the observation of a linear increase of the cell volume as x is increased (inset of figure 1). Using

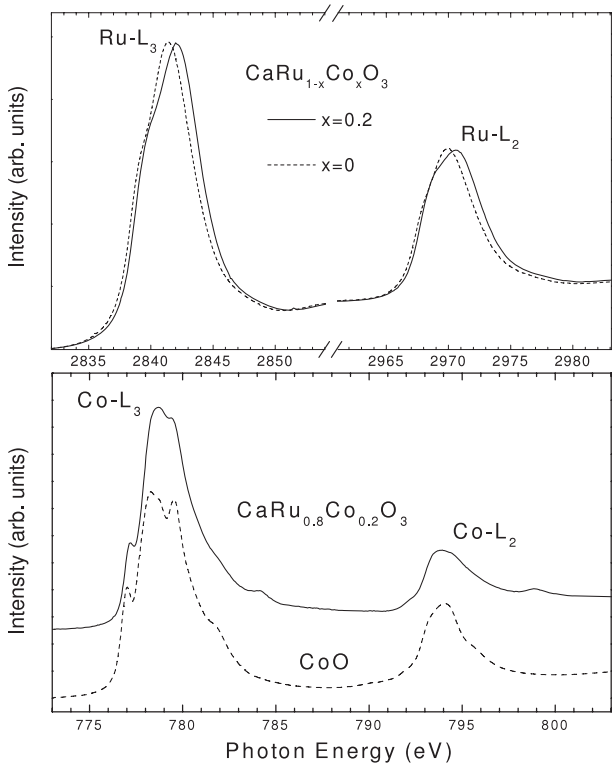

Figure 2. Top panel: Ru-$L_{2,3}$ XAS spectrum of $CaRu_{0.8}Co_{0.2}O_3$ (solid line), along with that of $CaRuO_3$ used as a Ru^{4+} reference (dashed line); bottom panel: Co-$L_{2,3}$ XAS spectrum of $CaRu_{0.8}Co_{0.2}O_3$ (solid line), along with that of CoO used as a Co^{2+} reference (dashed line).

tabulated ionic radii, volume variations were calculated for different types of charge transfer, corresponding to the three possible valence states of Co: (i) $Ru^{4+}_{1-x}Co^{4+}_x$; (ii) $Ru^{4+}_{1-2x}Ru^{5+}_xCo^{3+}_x$; (iii) $Ru^{4+}_{1-3x}Ru^{5+}_{2x}Co^{2+}_x$. The observed volume variation in $CaRu_{1-x}Co_xO_3$ directly points to the relevance of the charge transfer $Ru^{4+}_{1-3x}Ru^{5+}_{2x}Co^{2+}_x$, since it is the only one leading to a volume expansion with x. This can be ascribed to the relatively large size of Co^{2+} (0.0745 nm) compared with the other cations (Ru^{5+}: 0.0565 nm, Ru^{4+}: 0.0620 nm and Co^{3+}: 0.061 nm). Even quantitatively, it is worth noticing that the agreement is remarkable between the experimental variation and that expected for cobalt being in the divalent state.

EDS analyses coupled with electronic diffraction observations were performed on numerous crystallites of each compound. In all cases, the average cationic formula was found to be in good agreement with the nominal one, but it must be noted that there is always a scatter in the Ru/Co ratio which slightly differs from one crystallite to the other. For instance, the nominal $CaRu_{0.8}Co_{0.2}O_3$ compound corresponds to a distribution of local compositions $Ru_{(1-x)}Co_x$ with x varying between 0.18 and 0.25.

3.2. XAS

To investigate more directly the valence state of Ru and Co in $CaRu_{1-x}Co_xO_3$, x-ray absorption spectroscopy was performed at both the Ru-$L_{2,3}$ and Co-$L_{2,3}$ edges. The bottom panel of figure 2 displays the Co-$L_{2,3}$ XAS spectrum of $CaRu_{0.8}Co_{0.2}O_3$, along with that of CoO used as

a Co^{2+} reference. The spectra are dominated by the Co 2p core–hole spin–orbit coupling which splits the spectrum in two parts, namely the L_3 ($h\nu \cong 779$ eV) and L_2 ($h\nu \cong 794$ eV) white lines regions. The line shape of the spectrum at the 3d transition metal $L_{2,3}$ edges strongly depends on the multiplet structure given by the 3d–3d and 2p core–hole 3d Coulomb and exchange interactions, as well as the local crystal fields and the hybridization with the O 2p ligands. The dipole selection rules in the XAS spectrum are very effective in determining which of the $2p^5 3d^{n+1}$ final states can be reached and with what intensity, starting from a particular $2p^6 3d^n$ initial state. This makes the technique extremely sensitive to the symmetry of the initial state, i.e. the valence state [21] and the spin state [22–25] of the transition metal ions. In CoO, the cation Co^{2+} is well known to be in a high-spin state ($S = 3/2$). Since both the energy position and the multiplet structure are very similar in CoO and $CaRu_{0.8}Co_{0.2}O_3$, one can conclude that Co in the latter compound is in a high-spin divalent state. In order to obey the charge balance, the replacement of Ru ions by Co^{2+} ions must be accompanied by an increase in the valence state of Ru—most probably to Ru^{5+}. To further confirm this point, we turn to the Ru-$L_{2,3}$ XAS spectrum.

The top panel of figure 2 compares the Ru-$L_{2,3}$ XAS spectrum of $CaRu_{1-x}Co_xO_3$ for $x = 0.2$ and for $x = 0$, the latter compound being regarded as a Ru^{4+} reference. In the $L_{2,3}$ XAS spectrum of the 4d transition metals, the multiplet effects are much weaker than those of 3d transition metals. For the tetravalent Ru compound $CaRuO_3$, the main structures at 2841.3 eV in the Ru-L_3 edge and at 2969.9 eV in the Ru-L_2 edge basically correspond to the transition from the Ru 2p core level to the e_g-related state, while the shoulder at about 2 eV below the main peak is the transition to the t_{2g}-related state. The overall spectral feature is similar to that found in Sr_2RuO_4 and RuO_2 [26]. It was previously shown that the main peak is gradually shifted to higher energy when increasing the Ru valence. Typically, an increase in the valence of Ru from 4+ to 5+ results in a shift of the main peak to higher energy by 1.4 ± 0.2 eV [27]. Since Co is found to be divalent in $CaRu_{1-x}Co_xO_3$, the charge balance makes Ru to get a mean valence state $n = (4-2x)/(1-x)$. For $x = 0.2$, this leads to $n = 4.5$. In the top panel of figure 2, one observes a shift of the main peaks at both the Ru-L_3 and Ru-L_2 edges to higher energy by about 0.7 ± 0.1 eV for $x = 0.2$, which corresponds to a linear energy shift when increasing the mean Ru valency from 4+ up to 4.5+, in agreement with previous findings in $La_{2-x}Sr_xCu_{1-y}Ru_yO_4$ [27] and $SrRu_{0.5}Mn_{0.5}O_3$ [28]. Another signature of the increase in the Ru valency when x goes from 0 to 0.2 is the increased relative intensity of the t_{2g}-related shoulder structure (see top panel of figure 2). This behaviour was shown to be well reproduced by crystal-field-multiplet calculations involving an interplay between the 4d spin–orbit coupling and the multiplet interactions [26–28].

3.3. Magnetism

In the $CaRu_{1-x}Co_xO_3$ compounds, the reciprocal magnetic susceptibility as a function of temperature exhibits a linear regime at high-T, which extents over a substantial range below 300 K for $x \leqslant 0.3$. This behaviour corresponds to a Curie–Weiss law of the form $\chi = C/(T - \theta)$, where C is the Curie constant and θ is the Curie–Weiss temperature. The inset of figure 3 exemplifies this feature for $x = 0.1$. Fitting to the data within this paramagnetic regime allows us to extract θ and the effective number of Bohr magnetons, p_{eff}, using the practical relationship $p_{\text{eff}}^2 \simeq 8C$ (with C in cgs units). As displayed in the inset of figure 3, we emphasize that these parameters can be directly derived from the raw data, without requiring the introduction of a constant background χ_0. While θ does not show a systematic evolution with x (all values lie around -200 K), there is a monotonic increase in p_{eff} as x is increased, as shown in the main panel of figure 3. In line with most of the results of the literature [9, 12, 16],

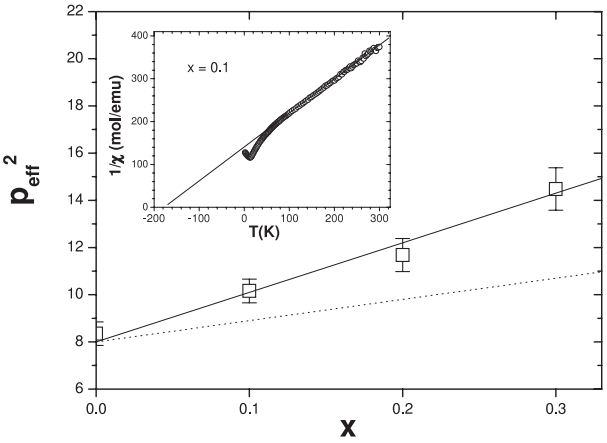

Figure 3. Main panel: experimental values of the effective number of Bohr magnetons in $CaRu_{1-x}Co_xO_3$ for $0 \leqslant x \leqslant 0.3$. Also shown are the expected values (see text) when considering Co^{2+} being either in a high-spin state (solid line) or in a low-spin state (dotted line). Inset: temperature dependence of the reciprocal susceptibility for $x = 0.1$. The solid line emphasizes the Curie–Weiss behaviour found at high temperatures.

we found only a slight difference between the experimental value of p_{eff} for $x = 0$ ($\simeq$2.9) and the Hund's rule value (2.83). Still within the framework of localized magnetism, one can predict the variation of p_{eff} with x, provided that the valence states of Co and Ru are known[4] According to the XAS study, the $CaRu_{1-x}Co_xO_3$ compounds contain divalent cobalt that is compensated by the appearance of ruthenium in the pentavalent state. This corresponds to the formula $Ca[Ru^{4+}_{1-3x}Ru^{5+}_{2x}]Co^{2+}_xO_3$, from which one deduces $p^2_{\text{eff}} = 8+21x$ when using the most likely values of spin state for each of the cations, namely the low-spin state for Ru^{4+} ($S = 1$) and high-spin state for both Ru^{5+} and Co^{2+} ($S = 3/2$). Note that the range of validity of such a formula ends at $x = 1/3$, a value above which Co must take a higher valence state—most probably Co^{3+}—to maintain the charge balance. In figure 3, one can see that the above formula of $p^2_{\text{eff}}(x)$ well accounts for the data for x up to 0.3 (solid line). For matter of comparison, we also plotted the results of the calculations for an hypothetical low-spin state of Co^{2+} ($S = 1/2$), which clearly departs from the data (dotted line).

The low-T magnetic susceptibility of $CaRu_{1-x}Co_xO_3$ is shown in figure 4 for $0 \leqslant x \leqslant 0.4$. The main panel displays the curve of $x = 0$ along with those of the pure Co-substituted compounds (i.e. $x = 0.1$ and 0.2). In accordance with the literature, the curve of $CaRuO_3$ continuously increases as T is decreased, reaching about 0.007 emu mol^{-1} at the lowest temperatures [4, 11]. The situation is qualitatively very different for the substituted compounds since their $\chi(T)$ curves clearly exhibit a peak in the low-T range. This peak is located close to 13 K for $x = 0.1$, and it is shifted up to 33 K for $x = 0.2$. For $x \geqslant 0.3$, the susceptibility curves get a more complex shape. As visible in the inset of figure 4, the most stringent feature of $\chi(T)$ remains the presence of a peak, but one can also detect a shoulder on the low-T side (at $\sim$20 K). It deserves to be noted that the appearance of this shoulder was found to correlate with the emergence of a small spontaneous magnetization around 60 K. Moreover, investigation of the series up to $x = 0.5$ revealed that both these features become more prominent as the fraction of secondary phase is increased. Therefore, one can consider that

[4] It must also be assumed that the samples remain stoichiometric in oxygen, which is reasonable in the present case considering that the syntheses are carried out in air.

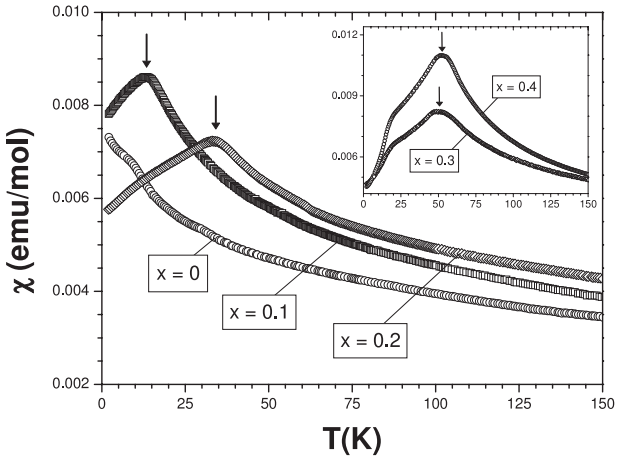

Figure 4. Temperature dependence of the magnetic susceptibility recorded in $CaRu_{1-x}Co_xO_3$, for a series of x values ranging from 0 to 0.4. The arrows mark the location of the peaks associated with freezing temperatures (see text).

this shoulder in $\chi(T \sim 20\ \mathrm{K})$ for $x \geqslant 0.3$ is not intrinsic to the $CaRu_{1-x}Co_xO_3$ phase, but is rather ascribable to the secondary phase. On the other hand, the peaks found in the $\chi(T)$ curves for $x \geqslant 0.3$ still exhibit the same features as those found in the pure compounds when $x < 0.3$ (in particular, the same type of frequency dependence as will be discussed below). This feature suggests that, for all investigated x values, the peak present in the $\chi(T)$ curves can be regarded as a property typical of the $CaRu_{1-x}Co_xO_3$ phase. Comparing to the literature, it is worth remarking that the locations of the peak for $x = 0.2$ ($\simeq$33 K) and $x = 0.3$ ($\simeq$50 K) are consistent with the study of He and Cava [14], who reported an anomaly slightly below 50 K for $x = 0.25$.

As already noticed, the presence of a peak in $\chi(T)$ is indicative of an SG behaviour, but it is not a proof in itself. To check the existence of a 'true' SG in $CaRu_{1-x}Co_xO_3$, we investigated in more detail one of these compounds, considering the highest x value that yields a pure compound, i.e. $x = 0.2$. Figure 5 compares different types of $\chi(T)$ curves recorded in $CaRu_{0.8}Co_{0.2}O_3$, focusing on the region of the peak. First of all, it can be noted that all curves—corresponding either to the dc or ac susceptibility—well coincide on the high-T side. As T is decreased, however, these curves separate from each other. Considering first the dc curves, one observes a peak in the ZFC curve, while the FC curve is almost flat below the temperature of this peak. We have already specified that this behaviour is one of the hallmarks of an SG [20]. Considering the ac curves, one observes that the location of the peak in $\chi'(T)$ is shifted to higher T as the frequency is increased, while its height is decreased. It must be emphasized that this is precisely the behaviour expected for a SG transition [20]. Quantifying the frequency dependence by the phenomenological parameter $K = (\Delta T_f/T_f)/\Delta \log(f)$, one obtains $K \simeq 0.017$ for $x = 0.2$. This value is in the range typical of spin-glass materials, i.e. 0.004–0.080 [20]. It is also the case of the larger x values (up to 0.5), for which rougher investigations yield $K \simeq 0.030 \pm 0.005$.

As underlined by Mydosh [20], an SG transition is characterized by other signatures which are less often investigated. For instance, in an SG, the temperature of the peak in $\chi'(T)$ must correspond to the inflection point on the high-T side of the $\chi''(T)$ maximum [29–31]. Figure 6 shows enlargements of the $\chi'(T)$ and $\chi''(T)$ curves of $x = 0.2$ in the region of the peaks. Despite the scatter in the χ'' data, the location of the maximum of $\chi'(T)$ is found to

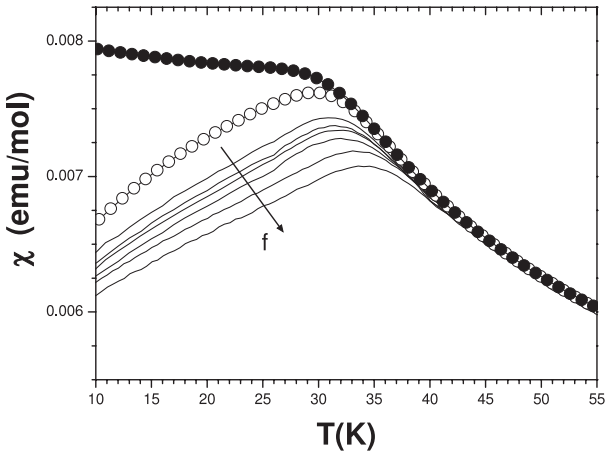

Figure 5. Enlargements of susceptibility curves of $CaRu_{0.8}Co_{0.2}O_3$ in the region of the peak. The empty and filled circles represent the dc susceptibility ($h_{dc} = 100$ Oe) recorded in the ZFC and FC modes, respectively. The solid lines are the real parts of the ac susceptibility ($h_{ac} = 10$ Oe) recorded with the frequency f equal to (from left to right): 10^{-1}, 10^0, 10^1, 10^2, 10^3 and 10^4 Hz.

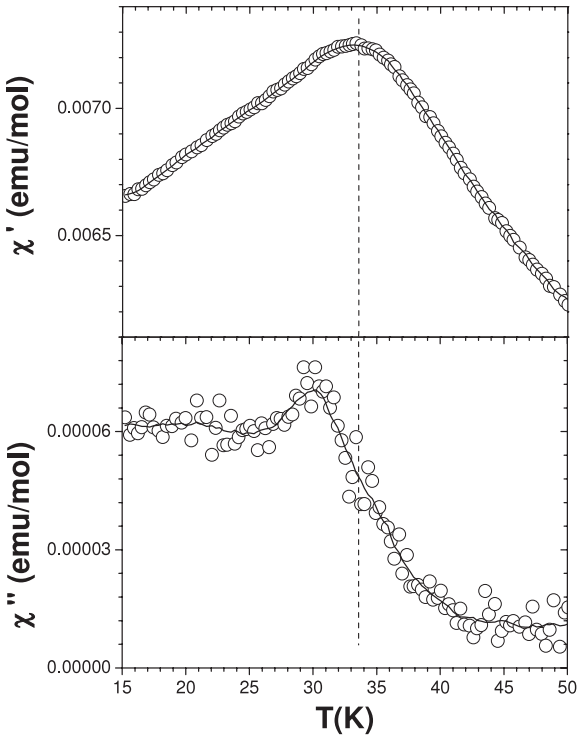

Figure 6. Comparison of the real and imaginary parts of the ac susceptibility of $CaRu_{0.8}Co_{0.2}O_3$ in the transition region ($h_{ac} = 10$ Oe; $f = 10^3$ Hz). The dotted line emphasizes the good agreement existing between the temperature of the maximum in χ' and that of the inflection point in χ''. The solid lines are 'smoothed' curves that are only guides to the eye.

be consistent with the midpoint of the increase in $\chi''(T)$ for decreasing temperature, another result which supports the SG nature of the transition.

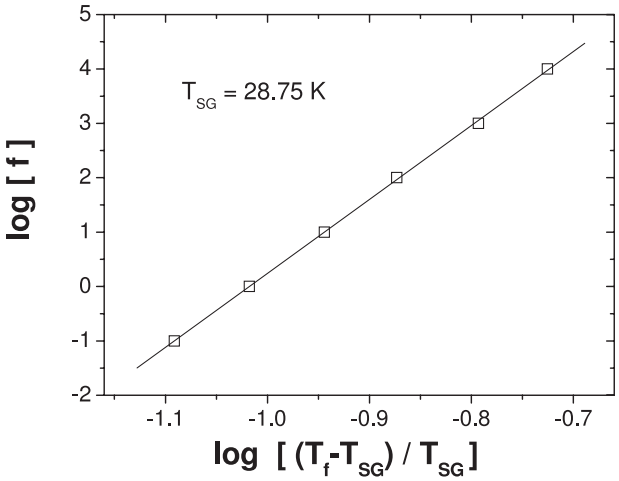

Figure 7. Frequency dependence of the freezing temperature of $CaRu_{0.8}Co_{0.2}O_3$ in the plot characteristic of the dynamical scaling model (see text). The figure displays the best fitting that corresponds to the following values of parameters: $T_{SG} = 28.75$ K; $f_0 = 6.9\,10^{13}$ Hz and $z\nu = 13.6$.

Still with the aim to test the achievement of an SG in $CaRu_{1-x}Co_xO_3$, one can analyse in more detail the frequency dependence of the glassy transition. This characteristic temperature is most often associated with the location of the peak in $\chi''(T)$. However, the frequency dependence of a freezing temperature T_f can also be tracked by considering the location of the peak in $\chi'(T)$ [30, 32, 33], which allows us to get a better resolution owing to the larger amplitude of the signal. Doing so in the case of $x = 0.2$, we can follow the frequency dependence of T_f over five decades.

The nature of the temperature and frequency dependence of T_f in a genuine SG has been the subject of intense debate in the last decades. However, the dynamic scaling theory [34] is generally admitted to be the most relevant to account for an SG transition [35]. This theory predicts a power law of the form $f = f_0(\frac{T_f - T_{SG}}{T_{SG}})^{z\nu}$, where f_0 is a characteristic attempt frequency, T_f is the frequency-dependent freezing temperature, T_{SG} is the underlying spin-glass transition, and $z\nu$ is a critical exponent. A good test for the relevance of this model consists in using the equivalent form:

$$\log(f) = \log(f_0) + z\nu \log\left(\frac{T_f - T_{SG}}{T_{SG}}\right).$$

We proceeded as follows: (i) first, the value of T_{SG} was adjusted in order to get the best linearity in a $\log(f)$ versus $\log\left(\frac{T_f - T_{SG}}{T_{SG}}\right)$ plot; (ii) then, $\tau_0 = 1/f_0$ and $z\nu$ were derived from the parameters of the linear fitting. The result of this procedure is shown in figure 7. One observes the existence of a remarkable linearity over five decades, which shows that the spin transition in $CaRu_{0.8}Co_{0.2}O_3$ well obeys the behaviour expected for an SG. The values of parameters corresponding to figure 7 are $T_{SG} = 28.75$ K, $\tau_0 = 1.4\,10^{-14}$ s and $z\nu = 13.6$. As expected in the dynamic scaling theory, the value of T_{SG} is close to the location of the maximum in the ZFC $\chi(T)$ curve. One can also notice that τ_0 lies within the range of values typical of spin glasses (10^{-10}–10^{-14} s) [32, 35]. As for $z\nu$, it is larger than the values of canonical spin glasses (5–10) [35, 36], but it remains consistent with the results of other types of spin glass, like for instance $Ho_5Co_{50}Al_{45}$ [38] and $La_{1-x}Ca_xMnO_3$ ($0 \leqslant x \leqslant 0.15$) [39].

Table 1. Nature of the magnetic coupling between adjacent B-sites of the perovskite $CaRu_{1-x}Co_xO_3$. Three types of super-exchange (SE) coupling can be encountered: weak antiferromagnetic (AF(w)), strong antiferromagnetic (AF(s)), and moderate ferromagnetic (FM(m)).

SE coupling	Ru^{4+}	Ru^{5+}	Co^{2+}	Co^{3+}
Ru^{4+}	w-AF	w-AF	m-FM	m-FM
Ru^{5+}	w-AF	w-AF	m-FM	m-FM
Co^{2+}	m-FM	m-FM	s-AF	s-AF
Co^{3+}	m-FM	m-FM	s-AF	s-AF

The overall magnetic investigation allows us to conclude that the substitution of Ru by Co in $CaRuO_3$ actually leads to the formation of an SG state. Let us now address the question of the origin of such a behaviour. One knows that the occurrence of an SG state requires two basic ingredients: (1) the presence of competing interactions, and (2) the existence of randomness in the spatial distribution of these interactions [20]. Like in most of oxides containing 4d elements, the magnetism of ruthenates is well known to be delicate since it often corresponds to situations lying at the borderline between the itinerant and localized pictures [5]. On general grounds, however, it is expected that the disorder introduced by substitutions (especially when using 3d elements like Co) tips the balance in favour of localized magnetism [11]. This turns out to be experimentally supported by the resistivity curves $\rho(T)$ of the Co-substituted compounds, which were found to show a pronounced semiconducting-like behaviour at low-T. For instance, even for the lowest Co content $x = 0.1$, the resistivity at 5 K reaches $\simeq 3\,10^{-2}$ Ω cm, i.e., about two orders of magnitude larger than in $CaRuO_3$.

Within the framework of localized magnetism, it can be easily demonstrated that substituting Co for Ru in $CaRuO_3$ leads to fulfilling the two above conditions for an SG state. Even if we limit ourselves to $x < 1/3$, the introduction of Co^{2+} leads to a series of new elemental couplings between the spins located at adjacent B-sites of the perovskite structure. While there is only one type of coupling in $CaRuO_3$ (i.e. Ru^{4+}–Ru^{4+}), there are six types of coupling in the substituted compounds, namely: Co^{2+}–Ru^{4+}, Co^{2+}–Ru^{5+}, Co^{2+}–Co^{2+}, Ru^{4+}–Ru^{4+}, Ru^{4+}–Ru^{5+}, and Ru^{5+}–Ru^{5+}. It must also be noted that these various types of bond are randomly distributed since the structural characterizations gave no indication of cationic ordering among the B-sites. For all above cationic couples, super-exchange is expected to be the predominant mechanism for the magnetic interactions. The results obtained by using the Goodenough rules [37] are shown in table 1. Note that we also considered the case of Co^{3+} to account for x up to 0.5. One observes that the valence states have no impact on the nature of the couplings. This allows to simplify the situation by considering that there are only three types of magnetic coupling: weak antiferromagnetism (w-AF) for all types of Ru/Ru pairs; strong antiferromagnetism (s-AF) for all types of Co/Co pairs; moderate ferromagnetism (m-FM) for all types of Ru/Co pairs. In conclusion, the basic ingredients for the existence of an SG are actually fulfilled in $CaRu_{1-x}Co_xO_3$, since there are antagonistic interactions that are randomly distributed.

It is even possible to go a bit further by noting that the occurrence of these different types of coupling is highly dependent on the x value. To evaluate the fraction of each type, one can simplify the problem as follows: first, one just takes into account the cubic lattice consisting of the B-sites of the perovskite structure; second, since the nature of the coupling does not depend on the valence states, it is sufficient to consider that each site of the lattice can be occupied either by Ru or by Co. Therefore, the fraction of each type of spin coupling is directly related to the probability of occurrence of the three possible configurations of adjacent sites

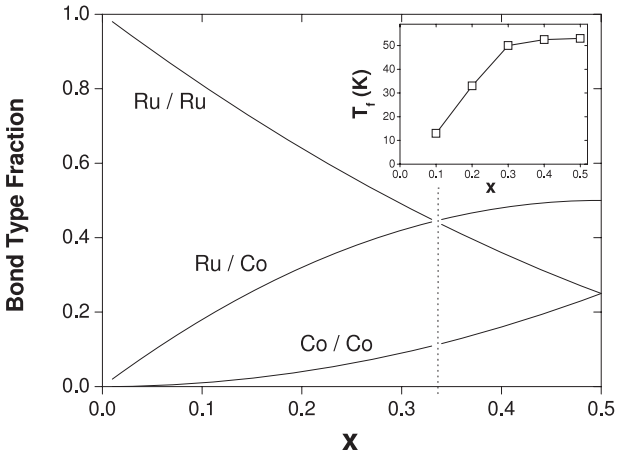

Figure 8. Main panel: probability of occurrence of the different types of B-site bonds in the perovskite $CaRu_{1-x}Co_xO_3$. The vertical dotted line marks the existence of a change in the valence states of Ru and Co: at the left, all data support the formula $Ca(Ru^{4+}_{1-3x}Ru^{5+}_{2x})Co^{2+}_xO_3$; at the right, Co^{3+} should appear, leading most likely to the formula $CaRu^{5+}_{1-x}(Co^{2+}_{1-2x}Co^{3+}_{3x-1})O_3$. The inset displays the x-dependence of the freezing temperature T_f (we considered here the maximum in $\chi'(T)$ for $f = 10^3$ Hz).

in the cubic lattice. It is found that the fraction of w-AF bonds (i.e. Ru/Ru) is $(1-x)^2$; the fraction of s-AF bonds (i.e. Co/Co) is x^2; the fraction of m-FM bonds (i.e. Ru/Co) is $2x(1-x)$. These fractions are plotted as a function of x in figure 8. It is worth noting that the super-exchange rules well account for the existence of competing interactions over the whole x range. Note, however, that the involved magnetic species change at $x = 1/3$. For instance, while the Ru/Co interactions involve Ru^{4+}–Co^{2+} and Ru^{5+}–Co^{2+} for $x < 1/3$, one must consider Ru^{5+}–Co^{2+} and Ru^{5+}–Co^{3+} for $x > 1/3$. Even though this makes no change in the nature of the interactions, the strengths of these couplings are probably modified. Roughly speaking, however, one can still consider that the 'degree of disorder in the interactions', from which derives the strength of the magnetic frustration, is maximum when the numbers of AF and FM bonds are equal to each other. In the present case, this situation simply corresponds to a fraction of Ru/Co bonds equal to 0.5 since it is the only type of FM interactions. In the inset of figure 8, one can observe that the evolution of the freezing temperature—which reflects the degree of magnetic frustration—indeed increases with x in a way similar to the fraction of Ru/Co bonds, tending to saturation when approaching $x = 0.5$.

Lastly, one can wonder whether the existence of an SG in the case of $M = Co^{2+}$ is consistent with the other results found in $CaRu_{1-x}M_xO_3$. Let us first emphasize that no systematic correlation has been reported so far between the nature of the substituting cation M and the type of magnetic state in $CaRu_{1-x}M_xO_3$. At the present time, there are eight cations M for which a well-identified magnetic state has been reported: (i) ferromagnetic state for Ti^{4+} [11–13], Fe^{3+} [12, 14, 15], Ni^{2+} [14], Mn^{4+} [14] and Cr^{3+} (or Cr^{4+}) [16, 17]; (ii) spin-glass state for Sn^{4+} [3], Cu^{2+} [19] and Co^{2+} ([14] and present study). On the one hand, it can be emphasized that the formation of an SG state with Co^{2+} is consistent with the result of Cu^{2+}, since both ions have the same basic features: they are divalent (creating a mixed valency Ru^{4+}/Ru^{5+}); they are magnetic (having $S = 3/2$ and $S = 1/2$, respectively); and they lead to a ferromagnetic M–Ru super-exchange coupling (for both Ru valence states). On the other hand, it is striking to observe that Ni^{2+} yields a ferromagnetic state, while this cation also shares

these features with Co^{2+} and Cu^{2+}. A possibility to account for this discrepancy would be the existence of an M–Ru coupling that is significantly stronger for $M = Ni^{2+}$ than for $M = Co^{2+}$ or $M = Cu^{2+}$. In this case, indeed, each M cation can polarize the nearest-neighbouring Ru spins, creating magnetic clusters which yield a macroscopic ferromagnetic-like behaviour. In such a situation—which was previously observed with Cr^{3+} and Fe^{3+}—the ferromagnetic fraction must have a maximum for x around 0.2 [14–17] It would be valuable to check this point in the case of Ni^{2+}, which has only been investigated up to $x = 0.05$ so far. Note that the possibility of such a phenomenon underlines the fact that the realization of an SG requires the presence of interactions that are not only of different signs but also of comparable strengths.

Still trying to classify the substitution effects in $CaRu_{1-x}M_xO_3$, one faces a problem with Sn^{4+}. Although it is completely different from Co^{2+} and Cu^{2+}, the cation Sn^{4+} was reported to yield an SG state [3]. This is a bit surprising since Sn^{4+} is a tetravalent non-magnetic cation which should essentially lead to a dilution effect, keeping Ru^{4+} as the only magnetic species. Therefore, the existence of mixed interactions—a necessary ingredient for an SG—is not obvious. We also remark that the existence of an SG limited to a narrow, intermediate range of concentration (i.e. 0.04–0.10 for Sn^{4+}) is quite unusual. Lastly, it is puzzling to get an SG state with Sn^{4+}, while this cation is very similar to Ti^{4+} which clearly leads to ferromagnetism [12–14]. This rapid review of the experimental situation—even without considering the cations leading to more complex behaviour—shows that the understanding of the substitution effects in $CaRu_{1-x}M_xO_3$ is still an open issue. It is also apparent that it would be desirable to re-investigate some of the previously studied cations in order to get a more comprehensive view of the experimental situation.

4. Conclusion

The effect of the substitution of Co for Ru in $CaRuO_3$ has been re-investigated in detail. We focused our study of $CaRu_{1-x}Co_xO_3$ on the range $x < 0.3$, which led to pure samples. Within this x range, the results of XRPD, XAS and measurements in the paramagnetic regime were shown to be consistent with the formula $Ca[Ru^{4+}_{1-3x}Ru^{5+}_{2x}]Co^{2+}_xO_3$. Investigation of the magnetic behaviour at lower temperature clearly points to the formation of a spin-glass state in $CaRu_{1-x}Co_xO_3$, a feature well attested by the frequency dependence of the ac susceptibility. It is shown that this substitution-induced magnetic ground state can be accounted for within the framework of localized magnetism. Comparison with the literature on $CaRu_{1-x}M_xO_3$ (M being a transition metal element) suggests that the strength of the super-exchange couplings would be a determinant factor controlling the nature of the magnetic state in this class of ruthenates.

Acknowledgment

We are grateful to Dr Z Hu for valuable discussion and experimental assistance.

References

[1] Longo J M, Raccah P M and Goodenough J B 1968 *J. Appl. Phys.* **39** 1327
[2] Gibb T C, Greatex R G, Greenwood N N and Kaspi P 1973 *J. Chem. Soc. (Dalton Trans.)* **12** 1253
[3] Cao G, McCall S, Bolivar J, Shepard M, Freibert F, Henning P, Crow J E and Yuen T 1996 *Phys. Rev.* B **54** 15–144
[4] Cao G, McCall S, Shepard M, Crow J E and Guertin R P 1997 *Phys. Rev.* B **56** 321
[5] Mazin I I and Singh D J 1997 *Phys. Rev.* B **56** 2556
[6] Kiyama T, Yoshimura K, Kosuge K, Michor H and Hilscher G 1998 *J. Phys. Soc. Japan* **67** 307

[7] Yoshimura K, Imai T, Kiyama T, Thurber K R, Hunt A W and Kosuge K 1999 *Phys. Rev. Lett.* **83** 4397
[8] Mukuda H, Ishida K, Kitaoka Y, Asayama K, Kanno R and Takano M 1999 *Phys. Rev.* B **60** 12–279
[9] Felner I, Nowik I, Bradaric I and Gospodinov M 2000 *Phys. Rev.* B **62** 11–332
[10] He T, Huang Q and Cava R J 2000 *Phys. Rev.* B **63** 024402
[11] He T and Cava R J 2001 *Phys. Rev.* B **63** 172403
[12] Felner I, Asaf U, Nowik I and Bradaric I 2002 *Phys. Rev.* B **66** 054418
[13] Hardy V, Raveau B, Retoux R, Barrier N and Maignan A 2006 *Phys. Rev.* B **73** 094418
[14] He T and Cava R J 2001 *J. Phys.: Condens. Matter* **13** 8347
[15] Mizusaki S, Taniguchi T, Okada N, Nagata Y, Hiraoka N, Nagao T, Itou M, Sakurai Y, Ozawa T C and Noro Y 2006 *Phys. Rev.* B **74** 052401
[16] Durairaj V, Chikara S, Lin X N, Douglass A, Cao G, Schlottmann P, Choi E S and Guertin R P 2006 *Phys. Rev.* B **73** 214414
[17] Maignan A, Raveau B, Hardy V, Barrier N and Retoux B 2006 *Phys. Rev.* B **74** 024410
[18] Cao G, Freibert F and Crow J E 1997 *J. Appl. Phys.* **81** 3884
[19] Bradaric I M, Felner I and Gospodinov M 2001 *Phys. Rev.* B **65** 024421
[20] Mydosh A J 1993 *Spin Glasses: An Experimental Introduction* (London: Taylor and Francis)
[21] Mitra C, Hu Z, Raychaudhuri P, Wirth S, Csiszar S I, Hsieh H H, Lin H J, Chen C T and Tjeng L H 2003 *Phys. Rev.* B **67** 092404
[22] van der Laan G, Thole B T, Sawatsky G A and Verdaguer M 1988 *Phys. Rev.* B **37** 6587
[23] Thole B T and van der Laan G 1988 *Phys. Rev.* B **38** 3158
[24] Cartier dit Moulin C, Rudolf P, Flank A-M and Chen C T 1992 *J. Phys. Chem.* **96** 6196
[25] Hu Z, Wu H, Haverkort M W, Hsieh H H, Lin H-J, Lorenz T, Baier J, Reichl A, Bonn I, Felser C, Tanaka A, Chen C T and Tjeng L H 2004 *Phys. Rev. Lett.* **92** 207402
[26] Hu Z, von Lips H, Golden M S, Fink J, Kaindl G, de Groot F M F, Ebbinghaus S and Reller A 2000 *Phys. Rev.* B **61** 5262
[27] Hu Z, Golden M S, Ebbinghaus S G, Knupfer M K, Fink J, de Groot F M F and Kaindl G 2002 *Chem. Phys.* **282** 451
[28] Sahu R K, Hu Z, Rao M L, Manoharan S S, Schmidt T, Richter B, Knupfer M, Golden M, Fink J and Schneider C M 2002 *Phys. Rev.* B **66** 144415
[29] Hüser D, Wenger L E, van Duyneveldt A J and Mydosh J A 1983 *Phys. Rev.* B **27** 3100
[30] Fisher I R, Cheon K O, Panchula A F, Canfield P C, Chernikov M, Ott H R and Dennis K 1999 *Phys. Rev.* B **59** 308
[31] Deac I G, Mitchell J F and Schiffer P 2001 *Phys. Rev.* B **63** 172408
[32] Gunnarsson K, Svedlindh P, Nordblad P, Lundgren L, Aruga H and Ito A 1988 *Phys. Rev. Lett.* **61** 754
[33] Cardoso C A, Araujo-Moreira F M, Awana V P S, Takayama-Muromachi E, de Lima O F, Yamauchi H and Karppinen M 2003 *Phys. Rev.* B **67** 020407(R)
[34] Hohenberg P C and Halperin B I 1977 *Rev. Mod. Phys.* **49** 435
[35] Souletie J and Tholence J L 1985 *Phys. Rev.* B **32** 516
[36] Fischer K H and Hertz J 1991 *Spin Glasses* (Cambridge: Cambridge University Press)
[37] Goodenough J B 1966 *Magnetism and the Chemical Bond* (New York: Wiley)
[38] Tholence J L 1984 *Physica* B **126** 157
[39] Laiho R, Lähderanta E, Salminen J, Lisunov K G and Zakhvalinskii V S 2001 *Phys. Rev.* B **63** 094405